Asian Journal of Pharmaceutical Technology & Innovation
ISSN: 2347-8810

Research Article

Clinical Applications and Anatomic Variation of Inferior Phrenic Arteries and their Branches by 64-Slice Spiral CT Angiographic Analysis

Mukesh Kumar Singh[1], Xu Chuanbin[1], Chunbin Zhang[3], Zhang Wu*[1], Meghna Mitali[2], Xiaoyi Liu[3]

Received on: 08-04-2017
Accepted on: 12-04-2017
Published on: 15-04-2017

Corresponding Author:

*** Zhang Wu**
Department of Radiology, Hospital of Jiamusi University,
Jiamusi City, Heilongjiang Province, China - 154002
Tel: 0086-15694549083

*Email Id- radio01hub@gmail.com

ABSTRACT

Objectives: The present study aims at determining the ability of 64-slice spiral CT angiographic analysis to identify the origin and distribution of both the left and right IPAs and its branches in normal and pathological cases.

Methods: Three hundred cases of normal healthy subjects aged 20-89 years (median age = 54 years) who received the 64-slice spiral CT of abdominal vessel two-stage contrast-enhanced from the First Affiliated Hospital of Jiamusi University from August 2015 to February 2016 were selected for the study. Then the bilateral origin of the IPA was recorded, diameter and performance were measured, and the obtained data was then compared with that of the normal group. The statistical analysis was done with the help of SPSS version 17.0 statistical software.

Results and Conclusion: In addition, the IPA is frequently reconstructed through several pathways, mainly through the retroperitoneal network. The study also aims to apply such findings to the clinical scenario of treating HCC. IPA with 64-slice spiral CT angiography can clearly show the normal anatomy and variation of IPA.

Key-words: 64-slice spiral CT, Post-processing techniques, Inferior phrenic artery, Gross anatomy, Hepatocellular carcinoma

Cite this article as:
Dr. Mukesh Kumar Singh, Xu Chuanbin, Chunbin Zhang, Zhang Wu, Meghna Mitali, Xiaoyi Liu, Clinical Applications and Anatomic Variation of Inferior Phrenic Arteries and their Branches by 64-Slice Spiral CT Angiographic Analysis, Asian Journal of Pharmaceutical Technology & Innovation, 05 (23); 55-65, 2017. www.asianpharmtech.com

[1]Department of Radiology, First Affiliated Hospital of Jiamusi University, Jiamusi City, Heilongjiang Province, China-154002
[2]National Medical College, Birgunj, Nepal
[3]College of Basic Medicine, Jiamusi University, Jiamusi City, Heilongjiang Province, China- 154007

INTRODUCTION

The inferior phrenic artery (IPA) is found to be the most common extrahepatic collateral route to hepatocellular carcinoma (HCC). In the medical history, surgery has been considered as the most preferred treatment strategy for HCC. However, in the case of the advanced stage of the tumor accompanied with hepatic scarring, surgery is avoided as the lesions are often inoperable at the time of diagnosis (1). A previous study showed that, unlike the parenchyma, the blood supply to the hepatic tumors is typically arterial, supplied by the portal vein (2). The variants of IPA, i.e., the right and left IPAs (RIPA and LIPA, respectively), act as the supply route to these malignant tumors. This is because both the variants constitute the neighboring hepatic segments and traverse the bare liver area (3,4).

The anatomical study of IPA (especially for RIPA and LIPA that represents half of the hepatic artery) is considered important for the interventiosnal radiologists (5). A previous study has stated the various attributes of the multislice spiral CT (MSCT) angiography like the large cover area, fast scanning speed, clear imaging, and 3D display from multiple angles. Thus, these characteristics are considered to be of great importance in the diagnosis and treatment of hepatic diseases (6).

The present study deals with the following research statements:

1. To explore the technical control of computed tomography angiography (CTA) of IPA in the 64-slice spiral CT (MSCT) and compare the different iodine concentrations of contrast agents and different post-processing visualizing techniques like multiple planar reconstruction (MPR), maximum intensity projection (MIP), and volume rendering (VR) for people with normal IPA origin.
2. To study the normal anatomy and the variation of IPA by MSCT angiography and measure the inner diameter of the IPA on the MIP images at a point about 5 mm away from the opening of the origin.
3. To analyze the angiographical and anatomical variations of IPA in order to explore its clinical value in HCC in the collateral blood supply.

MATERIALS AND METHODS

Patients

Normal groups: Three hundred cases (168 male cases, 132 female cases) of normal healthy subjects aged 20-89 years (median age = 54 years) who received the 64-slice spiral CT of abdominal vessel two-stage contrast-enhanced from the First Affiliated Hospital of Jiamusi University from August 2015 to February 2016 were selected for the study. The subjects were randomly divided into two groups: A and B (150 cases for each group). Group A received contrast media containing 300 mg iodine/ml, whereas group B received contrast media containing 370 mg iodine/ml. All the images derived from CT original images were reconstructed with the minimum slice of 0.75 mm and interval of 0.40 mm. Image post-processing was introduced with MPR, MIP, and VR. Then the display capabilities of three different kinds of three-dimensional reconstructions and different iodine concentrations of contrast agent of IPA and its branches were compared. The statistical performance of IPA and MSCT imaging techniques were evaluated for finding their bilateral origin. The selected IPA origin opened at about 5 mm at the regional context, and the inner diameter of IPA was measured on the MIP images.

Disease group: A retrospective analysis unveiled the complete image data of 96 cases of patients with HCC that showed the existence of 30 cases (21 males and 9 females) of the IPA in patients with collateral blood supply by MSCT processing. Then the bilateral origin of the IPA was recorded, diameter and performance were measured, and the obtained data was then compared with that of the normal group.

Statistical analysis

The statistical analysis was done with the help of SPSS version 17.0 statistical software. The measurement of the

diameter of the subject was expressed as ± s. For image evaluation, chi-square test was used (test a = 0.05). P < 0.05 was considered statistically significant. To find the IPA diameter for the normal and disease group, independent samples t test was done.

Examination methods

All the patients drank pure water (500-1000 ml) and lay supinely on the scan table, head first body position. The scan range was from the top of the diaphragm to the lower pole of kidney. Image acquisition was done in a single breath-hold. CT enhanced scan contrast agent was heated up to 37°C, using a high pressure 20 gauge syringe through an ante-cubital vein of the right elbow vein injection speed of 4.0 ml/s, with 1.5 ml/Kg weight to calculate the required amount of contrast agents in the patients. The resulting original scanned image was with a minimum thickness of 0.75 mm, and 0.40 mm of spacing layer gap through the thin layer reconstruction image was present for the maximum view of IPA.

Equipments used in the study:

- CT examination scanner: Siemens Somation Sensation 64-slice CT machine.
- Image post-processing workstation: Syngo CT 2007s.
- Host Operating System: SIEMENS-MMWPE27A system

RESULTS AND DISCUSSION

In Group A, four cases showed no clear arterial enhancement and two cases showed a less clear origin for IPA. In addition, the display rate was 98%, and the excellent significant rate was 17.12%. In group B, 100% arterial enhancement was observed, with an excellent penetrance of 23.89%. For each group, three kinds of post-processing techniques, i.e., MPR, MIP and VR, were used for displaying the IPA origin and evaluating the ability of the gross anatomy. It was found that the differences were not statistically significant (group A: (χ^2 = 2.27, P > 0.05; group B: (χ^2= 9.43, P > 0.05)). Both the groups showed different significance (χ 2 = 10.30, P < 0.05) for the three kinds of post-processing techniques. In addition, the IPA origin and the gross anatomy of the ability of the difference were not statistically significant (χ^2=4.54，P>0.05).

The origins of the IPA branches in the normal groups of 300 cases of 594 subjects with a display rate of 99% are as follows (Fig. 1A-G). The IPA branches originated from the celiac axis in 50.51% of patients (300 of 594), abdominal aorta main arteries in 35.02% (208), the renal artery in 9.43% (56), the left gastric artery in 3.37% (20), the adrenal artery in 1.18% (7), the hepatic artery in 0.34% (2), and from the splenic artery in only 1% (1). Comparatively, the disease group showed a clear display of 60 IPA, of which 24 (40%) originated from the celiac trunk, 22 (36.67%) from the abdominal aorta, 10 (16.67%) from the renal artery, 3 (5%) from the renal artery, and 1 (1.67%) from the left gastric artery (Fig. 2A-E).

In the normal group, the average value of IPA diameter for the right side was 1.41 ± 0.3 mm, with 95% confidence interval (1.41 ± 0.04 mm). The left IPA diameter was 1.30 ± 0.37 mm, with 95% confidence interval (1.30 ± 0.04 mm). The right side IPA diameter was found to be significantly greater than the left side (t = 3.78, P <0.05). In the disease group, the right IPA diameter was 2.13 ± 0.75 mm, with 95% confidence interval (2.13 ± 0.28 mm), and the left IPA diameter was 1.56 ± 0.40 mm, with 95% confidence interval (1.56 ± 0.15 mm). The right side IPA diameter was found to be significantly greater than the left side (t = 3.48, P < 0.05). It was also found that the left and right ipsilateral IPA diameters for the disease group were significantly greater than that of the normal group (t = 3.63, 5.04; P < 0.05).

The normal variability and origin of IPA after using the post-processing techniques for both the groups, A and B, are shown in Table 1.

Table 1. Group A and Group B shows three kinds of reconstruction results for IPA branch and their comparison result

A*					B#				
Method	Evaluation			Total	Method	Evaluation			Total
	Excellent	Good	Qualified			Excellent	Good	Qualified	
MPR	45	83	166	294	MPR	62	90	148	300
MIP	49	88	157	294	MIP	78	86	136	300
VR	57	85	152	294	VR	75	93	132	300
Total	151	256	475	882	Total	215	263	416	900

Group	Three kinds of reconstruction^			Total
	Excellent	Good	Qualified	
Group A	151	256	476	882
Group B	215	263	416	900
Total	366	519	892	1782

* χ^2 =2.27, P>0.05; multiple planar reconstruction (MPR), maximum intensity projection (MIP) and volume rendering (VR)

χ^2 =9.43, P>0.05; multiple planar reconstruction (MPR), maximum intensity projection (MIP) and volume rendering (VR)

^ χ^2 =10.30, P<0.05

Table 2. The occurrence of normal IPA in 300 cases, and its origin of variation in percentage of IPA branches

Site of origin	Left IPA	Right IPA	Total
Celiac	187（63.61%）	113（37.67%）	300 (50.51%)
Abdominal aorta	93（31.63%）	115（38.33%）	208 (35.02%)
Left gastric artery	11 (3.74%)	9（3.00%）	20 (3.37%)
Renal artery	—	56（18.67%）	56 (9.43%)
Renal artery	2 (0.68%)	5（1.67%）	7 (1.18%)
Hepatic artery	—	2（0.67%）	2 (0.34%)
Splenic artery	1 (0.34%)	—	1 (0.17%)

Table 3. Thirty patients suffering from liver cancer and their originated IPA occurrence

Site of origin	Left IPA	Right IPA	Total
Celiac	17 (56.67%)	8 (26.67%)	25 (41.67%)
Abdominal aorta	11 (36.67%)	12 (40.00%)	23 (38.33%)
Renal artery	2 (6.67%)	8 (26.67%)	10 (16.67%)
Renal artery	—	1（3.33%）	1（1.67%）
Left gastric artery	—	1（3.33%）	1（1.67%）

Table 4. IPA diameter measurement between the normal and disease group（x±s）

Group (n)	Left IPA（mm）	Right IPA (mm)	T value	P value
Normal group（300）	1.30±0.37	1.41 ± 0.33	3.78	*P*<0.05
Disease group（30）	1.56±0.40	2.13 ± 0.75	3.48	*P*<0.05
T value	3.63	5.04	—	—
P value	*P*<0.05	*P*<0.05	—	—

In 594 normal display IPA cases, the origin of variation in the incidence of IPA is shown in Table 2. The IPA is found in the form of round or nodular high density along the MSCT cross section, with coronal reconstruction display along both sides of the oblique abdominal aortic lines like the vascular image.

The powerful data processing by the MSCT angiography advanced scanning technology can clearly show the relationship between blood vessels and the surrounding abdominal organs, keeping in view the clinical suspicion of aortic 3D shape of pseudo aneurysms, aortic dissection, aortic intramural hematoma, and aortic congenital vascular disease. Interventional radiology is needed for obtaining further image information. Such an intervention results in a more intuitive, precise, broader, and improved vascular examination techniques and clinical value of abdominal imaging, especially to meet the clinical microsurgery requirements (4, 7-11). Currently, MSCT angiography is a fast, accurate, and non-invasive pre-clinical diagnostic and surgical technique for the abdominal vascular emergencies (12-16). The potential clinical significance is established by the normal reference values.

In the present study, 300 cases of normal people were subjected to MSCT angiography, and the IPA's overall display rate was 99.33%. We believe that the origin of IPA on display rate of MSCT main factors is associated with the following properties: (1) The concentration of iodine contrast agent is not enough, and the difference seen in patients, especially on the left IPA diameter < 0.5 mm, was difficult to identify with naked eyes. (2) IPA close to the celiac origin when opening the abdominal aorta exhibited similarly between the origins of celiac or abdominal aorta. (3) Due to the complexity of IPA origin, the familiarity of IPA with the surrounding anatomical structures can also have an impact on the relationship between correct identification of IPA and its measurement. Therefore, this set of experiments resulted in a high concentration of contrast agent (370 mgI/ml) of the IPA that shows a more standard iodine contrast agent concentration (300 mgI/ml), which was found to be statistically significant. A greater degree of anatomical adjacent and relationship with IPA is exhibited by the thickness of the arterial line of the raw data (0.75 mm) and the reconstruction interval of 0.4 mm with the powerful post-processing capabilities that will significantly improve the display rate (17- 20).

MSCT three post-processing image display case of IPA and its major branches

Based on the observations of 300 cases subjected to multi slice spiral CT angiography with three reconstruction imaging techniques, there were no significant differences observed between the three displays ($P>0.05$ for both the groups). This means the high concentration of iodine contrast agent is superior to the standard display of the IPA (21-24). We found that the MPR images with a high ability to distinguish details seemed to be less demanding on the concentration of contrast agent that can be tracked at any level to observe the inner lumen of IPA and adjacent relationship with the surrounding circumstances from different angles of MIP images, adjusting the thickness of a reasonably clear and precise display of IPA. Vascular origin in general courses, high contrast, can accurately measure the IPA vessel diameter but lack space for visualizing 3D images. However, VR can generate 3D images of the IPA and peripheral vascular arteries and further establish an anatomical relationship of various tissues appearing to maximize the smooth tissue component of the vessel wall that appears with particular clarity at the image level. In short, the advantages of 64-slice CT post-processing approach include not increasing the amount of radiation and shortening of the examination time or three-dimensional reconstruction. Therefore, in the process of dimensional reconstruction of IPA, a different purpose post-processing method needs to be selected based on the observations and comprehensive application of various post-processing technology that will greatly enrich the MSCT display capabilities of the IPA (25-28).

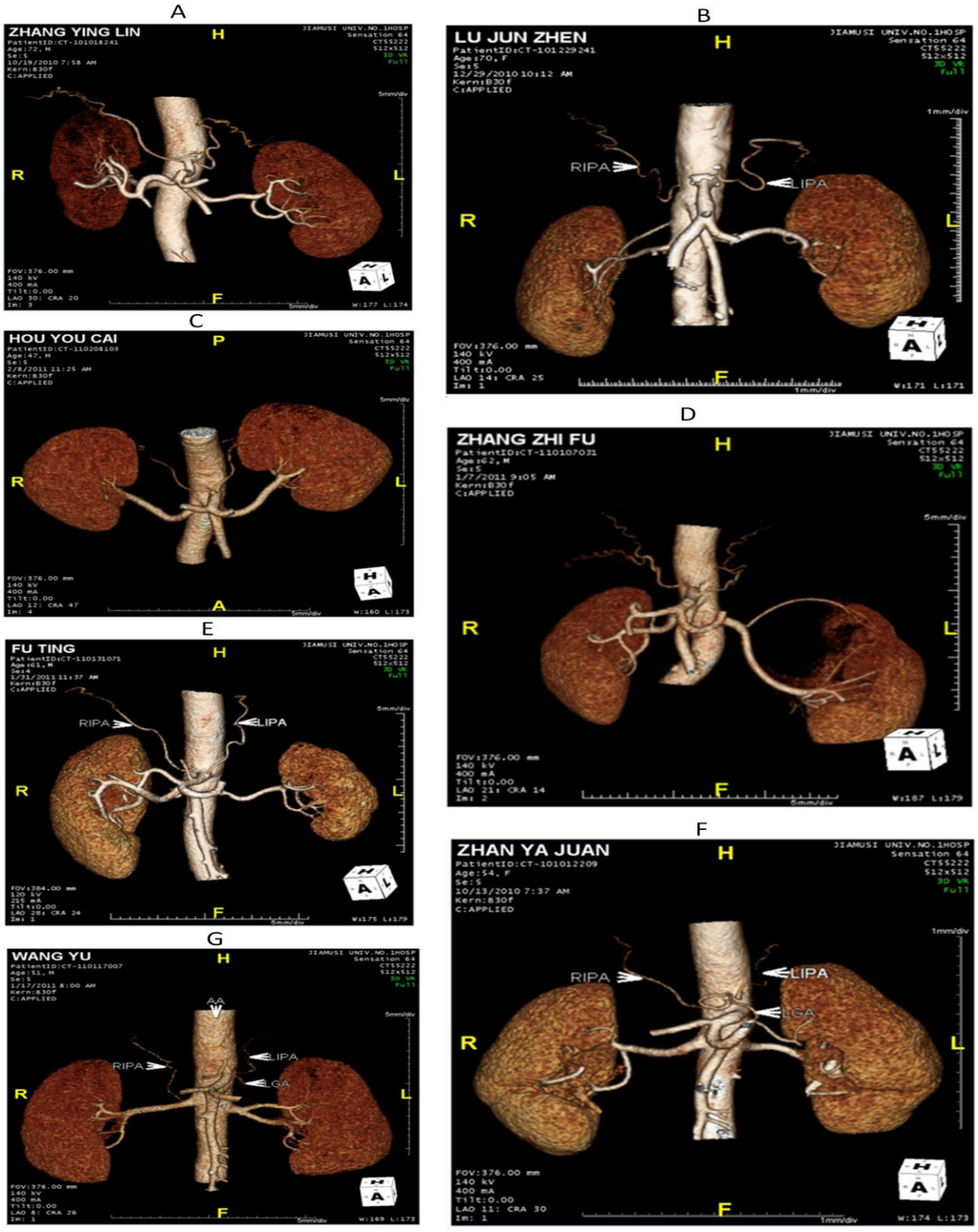

Figure 1: (A) RIPA and LIPA have dried in the origin of abdominal aorta; (B) Origin of RIPA and LIPA, respectively from the abdominal aorta; (C) RIPA and LIPA stems originated from the celiac trunk; (D) Origin of RIPA and LIPA from the celiac; (E) RIPA originates from the abdominal aorta, and the LIPA originates from the celiac; (F) RIPA left gastric artery origin, origin of LIPA abdominal aorta; (G) RIPA right renal artery origins, origin of LIPA left gastric artery

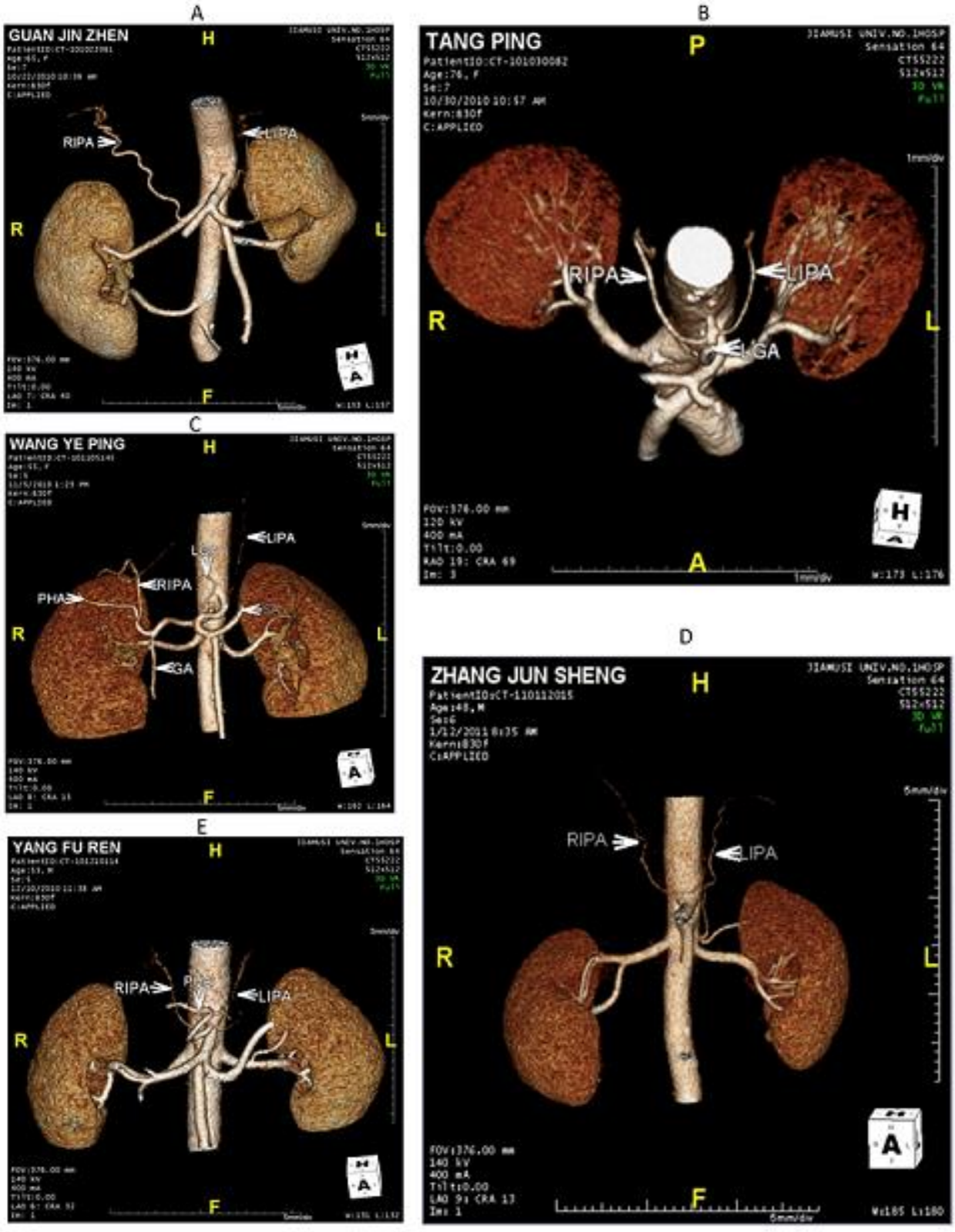

Figure 2: (A) Origin of RIPA from the right renal artery, LIPA origin of the celiac; (B) Origin of RIPA and LIPA, respectively from the left gastric artery; (C) Origin of RIPA was in hepatic artery, LIPA origins of the splenic artery; (D) Origin of RIPA abdominal aorta, LIPA origin from the left renal artery; (E) RIPA origin of hepatic artery, LIPA origin of the celiac

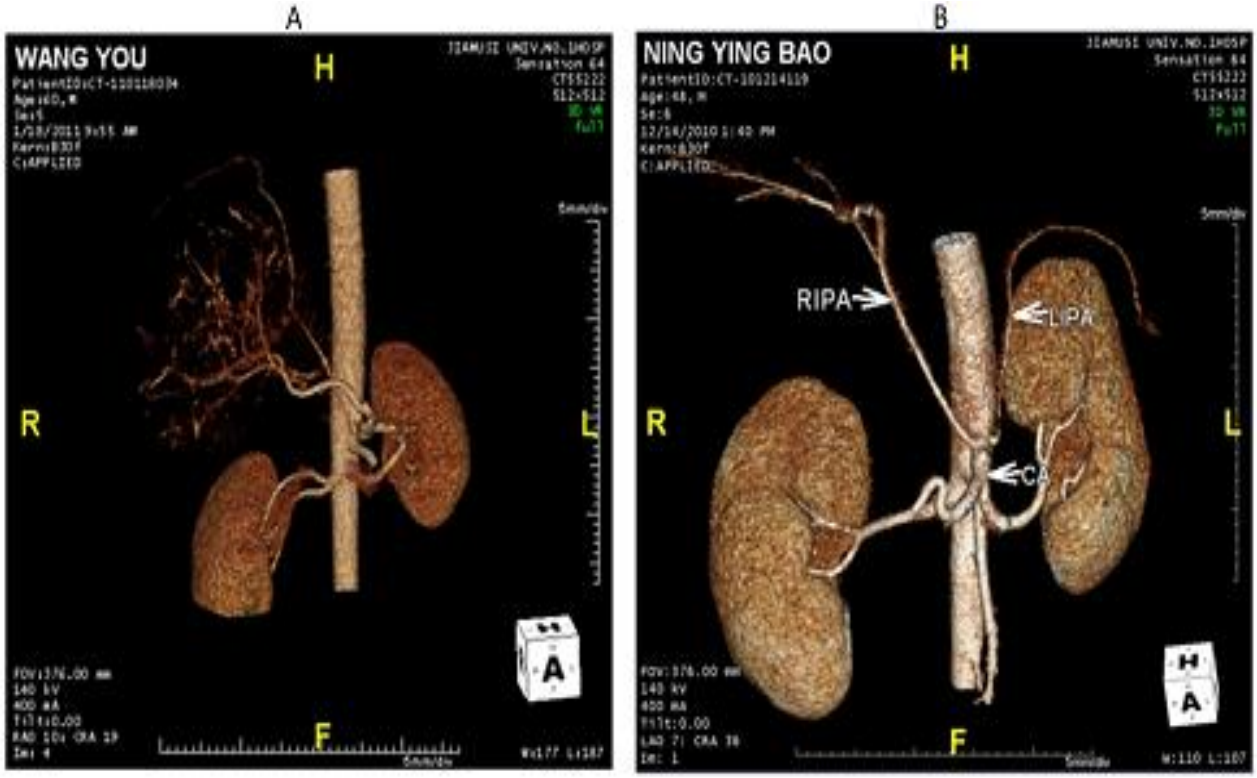

Figure 3: (A) Diseased group: RIPA origins of abdominal aorta, and see little blood supply of liver cancer; (B) Diseased group: RIPA thickened, branching increased form

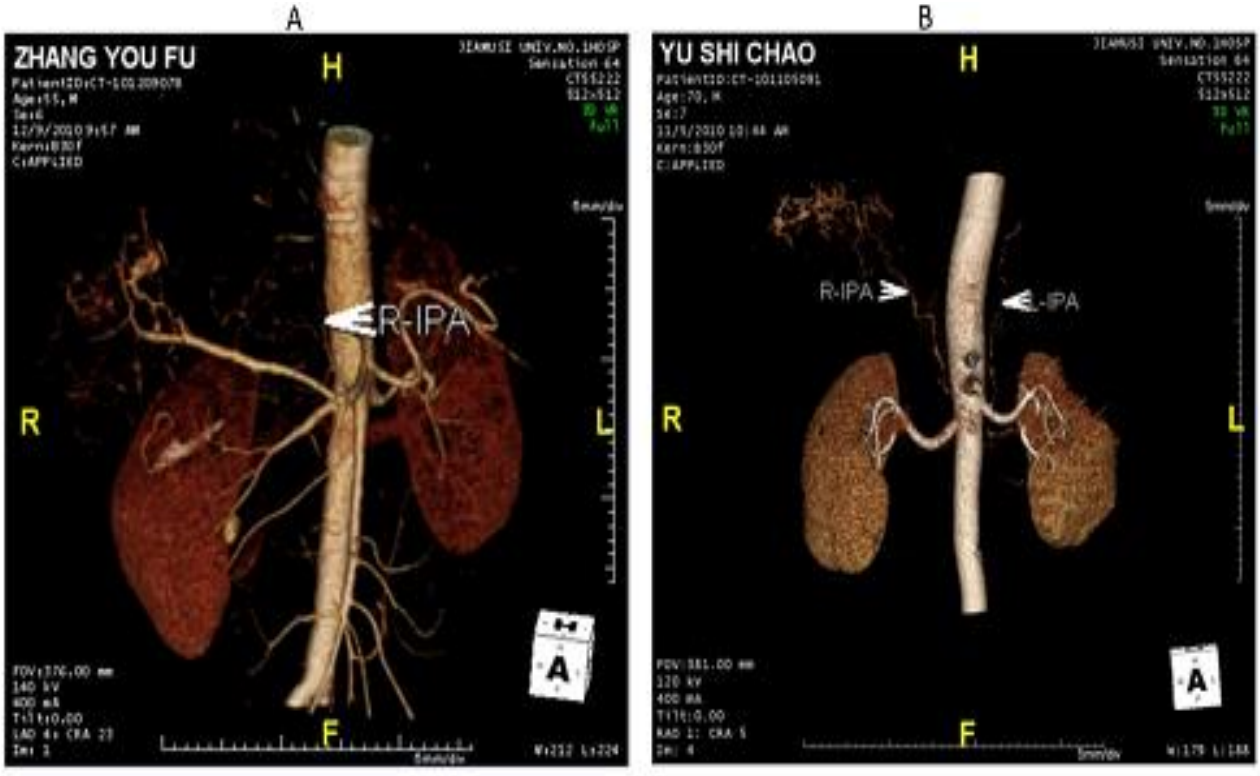

Figure 4: (A) Patients with hepatocellular carcinoma, RIPA blood supply of liver cancer; (B) Patients with hepatocellular carcinoma, hepatic tumor blood supply of RIPA

Origin of the IPA diameter with MSCT performance

The most common IPA origin was at the level of about 1 cm from the abdominal aorta vessel wall, both from the left and right sides, which were symmetrical. IPA also originated from the celiac artery and superior and inferior mesenteric artery. The RIPA and LIPA both originated from a common trunk. RIPA originating from the bottom of renal artery, left gastric artery, hepatic artery and splenic artery is rare (29, 30). The study found that the average diameter of the RIPA (1.41 ± 0.04 mm) was significantly larger than the left side (1.30 ± 0.04 mm) ($t = 3.78$, $P < 0.05$).

In a study conducted by Loukas et al. (10), 30 patients with HCC autopsy of the right IPA origin in celiac accounted for 40%, abdominal aorta 38%, renal artery 3%, left gastric artery 3% and hepatic artery 2%. In addition to this, the patients with HCC were treated with MSCT display IPA with similar origins, which were located in the right lobe of the liver cancer lesion, and the diameter was measured as 6.7 ± 1.5 cm. In patients with liver cancer, the IPA origin was celiac artery in 41.67% (25 cases), abdominal aorta in 38.33% (23 cases), and renal artery in 16.67% (10 cases). Further, the MIP imaging technique measured the mean diameter of RIPA at 2.13 ± 0.75 mm, with 95% confidence interval (2.13 ± 0.28) mm. It was significantly larger than the LIPA diameter 1.56 ± 0.40 mm, with 95% confidence interval (1.56 ± 0.15) mm, ($t = 3.48$, $P < 0.05$) (Table 4; Fig. 4A and B).

In recent years, scholars have found that IPA has important practical significance in terms of not only diagnosis and treatment of liver cancer. The IPA, esophagus-gastric branch, adrenal gland-renal artery in the lower esophagus, gastric cancer, kidney tumor and retroperitoneal space tumors are also of significance. Research in this area is not deep enough, and its potential link still requires further study.

We thus conclude that:

1. The two different iodine concentrations of contrast-enhanced scan of IPA shows significant differences. The high concentration of iodine contrast agent (370 mgI/ml) of the IPA's display is better than the standard iodine concentration of contrast agent (300 mgI/ml).
2. The comparison of 64-slice spiral CT three reconstructions (MPR, MIP, and VR), the IPA origin, and the gross anatomy of the ability to display results indicated that the three kinds of approach were not statistically significant. The 64-slice spiral CT post-processing techniques have their own advantages and disadvantages; therefore, they should be used in combination. The gross anatomy and three-dimensional structure were estimated with the space adjacent to the vascular organ.
3. IPA with 64-slice spiral CT angiography can clearly show the normal anatomy and variation of IPA and measured the IPA inner diameter of the normal reference range in order to provide imaging evidence for angiography and surgery.
4. The review of IPA by 64-slice spiral CT angiography analysis of disease group indicated that the 64-slice spiral CT leads to multi-angle observation. IPA is involved in blood supply to the liver tumors for the interventional treatment, clinical surgery, and liver transplantation.

Acknowledgments

The authors are grateful to all the professors and doctors of Department of Radiology, First Affiliated Hospital of Jiamusi University for their generous support.

REFERENCES

1. Yamada R, Sato M, Kawabata M, Nakatsuka H, Nakamura K, Takashima S. Hepatic artery embolization in 120 patients with unresectable hepatoma. Radiology 1983;148:397-401.

2. Chuang VP, Wallace S. Hepatic artery embolization in the treatment of hepatic neoplasms. Radiology 1981;140:51-8.
3. Duprat G, Charnsangavej C, Wallace S, Carrasco CH. Inferior phrenic artery embolization in the treatment of hepatic neoplasms. Acta Radiol 1988;29:427-9.
4. Kim HC, Chung JW, An S, Seong NJ, Jae HJ, Cho BH, Park JH. Left inferior phrenic artery feeding hepatocellular carcinoma: angiographic anatomy using C-Arm CT. Am J Roentgenol 2009;193:W288-94.
5. Gürses IA, Gayretli O, Kale A, Öztürk A, Usta A, Şahinoğlu K. Inferior Phrenic Arteries and Their Branches, Their Anatomy and Possible Clinical Importance: An Experimental Cadaver Study. Balkan Med J 2015;32:189-95.
6. Huang JH, Fan WJ, Li CJ, Gu YK, Zhang L, Gao F, Lu LW, Li WQ. Application of multislice spiral CT angiography on transcatheter arterial chemoembolization for hepatocellular carcinoma. Ai Zheng 2009;28:159-63.
7. Cheng YD. Common problems in chemotherapy and embolization through arterial perfusion for liver cancer. Journal of Interventional Radiology (Chinese) 1999;8:187-8.
8. Gokan T, Hashimoto T, Matsui S, Kushihashi T, Nobusawa H, Munechika H. Helical CT demonstration of dilated right inferior phrenic arteries as extra hepatic collateral arteries of hepatocellular carcinoma. J Comput Assist Tomogr 2001;25:68-73.
9. Kim HC, Chung JW, Lee W, Jae HJ, Park JH. Recognizing extra hepatic collateral vessels that supply hepatocellular carcinoma to avoid complications of trans catheter arterial chemoembolization. Radiographics 2005;25:S25-9.
10. Loukas M, Hullett J, Wagner T. Clinical anatomy of the inferior phrenic artery. Clin Anat 2005;18:357-65.
11. Zeng XH, Wang SZ, Wei CJ. The clinical efficacy of hepatic artery infusion chemotherapy and chemoembolization in the treatment of liver matastases. Chinese Journal of Oncology (Chinese) 1996;2:365-7.
12. Ito K, Kim MJ, Mitchell DG, Honjo K. Inferior phrenic arteries: depiction with thin-section three-dimensional contrast-enhanced dynamic MR imaging with fat suppression. J Magn Reson Imaging 2001;113:201-6.
13. Okino Y, Kiyosue H, Matsumoto S, Takaji R, Yamada Y, Mori H. Hepatocellular carcinoma: prediction of blood supply from right inferior phrenic artery by multiphasic CT. J Comput Assist Tomogr 2003;27:341-6.
14. Rosse C, Gaddum-Rosse P. Hollinshead's Textbook of anatomy. Philadephia: Lippincott-Raven; 1997.
15. Thunder LC, Advances in imaging of anatomic variations of the inferior phrenic arteries. Chinese Journal of Interventional Imaging and Therapy 2010;7:587-90.
16. Zhang N. Observation on 220 cases of inferior phrenic artery type. Anatomy 1958;3:203-9.
17. Matoba M, Tonami H, Kuginuki M, Yokota H, Takashima S, Yamamoto I. Comparison of high resolution contrast-enhanced 3D-MRA with digital subtraction angiography in the evaluation of hepatic arterial anatomy. Clin Radiol 2003;58:463-8.
18. Qi Chun thick, Lu Chuan, Liuzuoqin. C-arm CT in interventional therapy and its clinical application. International Journal of Medical Radiology 2008;31:359-61.
19. Tanaka R, Ibukuro K, Akita K. The left inferior phrenic artery arising from left hepatic artery or left gastric artery: radiological and anatomical correlation in clinical cases and cadaver dissection. Abdom Imaging 2008;33:328-33.
20. Virmani S, Ryu RK, Sato KT, Lewandowski RJ, Kulik L, Mulcahy MF, Larson AC, Salem R, Omary RA. Effect of C-arm angiographic CT on transcatheter arterial chemoembolization of liver tumor. J Vasc Interv Radiol 2007;18:1305-9.

21. Fenchel S, Fleiter TR, Aschoff AJ, van Gessel R, Brambs HJ, Merkle EM. Effect of Iodine Concentration of Contrast Media on Contrast Enhancement in Multi slice CT of the Pancreas. Br J Radiol 2004;77:821-30.
22. Itoh S, Ikeda M, Achiwa M, Satake H, Ota T, Ishigaki T. Multiphase Contrast-enhanced CT of the liver with a Multi slice CT Scanner: Effects of Iodine Concentration and Delivery Rate. Radiat Med 2005;23:61-9.
23. Jin C, Gang C, Dong W. Strengthening of different iodine concentration contrast medium on the aorta. Journal of Medical Radiation Technology 2007;5:2-4.
24. Yinghe Z, Wanchang T, Xiao-Hui L. Multi slice spiral CT angiography of right inferior phrenic artery. Journal of Interventional Imaging and Therapy 2008;5:433-6.
25. Haage P, Schmitz-Rode T, Hubner D, Piroth W, Günther RW. Reduction of contrast material dose and artifacts by a saline flush using a double-power injector in helical ct of the thorax. Am J Roentgenol 2000;174:1049-53.
26. Hopper KD, Mosher TJ, Kasales CJ, TenHave TR, Tully DA, Weaver JS. Thoracic spiral CT: delivery of contrast material pushed with injectable saline solution in a power injector. Radiology 1997;205:269-71.
27. Morcos SK, Thomsen HS, Webb JAW, Members of Contrast Media Safety Committee of the European Society of Urogenital Radiology (ESUR). Contrast media induced nephrotoxicity: a consensus report. European Radiology 1999;9:1602-13.
28. Yang X, Zhao L, Shujie C. Sub-clavian artery stenosis CTA examination contrast agent injection site and the speed of delivery. J Pract Nurs 2007;230:44-5.
29. Morcos SK, Thomsen HS, Webb JA. Contrast-media-induced nephrotoxicity: a consensus report. Contrast Media Safety Committee, European Society of Urogenital Radiology (ESUR). Eur J Radiol 1999;9:1602-13.
30. Williams PL. Gray's Anatomy. London: Churchill Livingstone; 1995.